MAN/HEP/2012/12

# An AdS/QCD holographic wavefunction for the $\rho$ meson and diffractive $\rho$ meson electroproduction

J. R. Forshaw

*Consortium for Fundamental Physics,*

*School of Physics & Astronomy, University of Manchester,*

*Oxford Road, Manchester M13 9PL, U.K.**

R. Sandapen

*Département de Physique et d'Astronomie,*

*Université de Moncton, Moncton, N-B. E1A 3E9, Canada.*†



We show that AdS/QCD generates predictions for the rate of diffractive $\rho$-meson electroproduction that are in agreement with data collected at the HERA electron-proton collider.

## INTRODUCTION

To date, the correspondence between string theory in five-dimensional anti-de Sitter (AdS) space and four-dimensional QCD has enjoyed a number of successes (see [1–4] and references therein). In this letter, we demonstrate another success by showing that parameter-free AdS/QCD wavefunctions for the $\rho$ meson lead to predictions for the rate of diffractive $\rho$ meson production ($\gamma^* p \to \rho p$) that agree with the data collected at the HERA $ep$ collider.

In previous papers [5, 6], we took a phenomenological approach and extracted the light-front wavefunctions of the $\rho$ meson using the HERA data. We follow the same formalism here, except that we now use the AdS/QCD wavefunctions predicted in [7, 8].

## THE ADS/QCD WAVEFUNCTION

Brodsky and de Téramond have recently shown that, in what they call a first semiclassical approximation to light-front QCD [9], the meson wavefunction can be written in the following

factorized form

$$\phi(x,\zeta,\varphi) = \frac{\Phi(\zeta)}{\sqrt{2\pi\zeta}} f(x) \mathrm{e}^{iL\varphi} \tag{1}$$

where $L$ is the orbital quantum number and $\zeta = \sqrt{x(1-x)}b$ ($x$ is the light-front longitudinal momentum fraction of the quark and $b$ the quark-antiquark transverse separation). The function $\Phi(\zeta)$ satisfies a Schrödinger-like wave equation

$$\left(-\frac{\mathrm{d}^2}{\mathrm{d}\zeta^2} - \frac{1-4L^2}{4\zeta^2} + U(\zeta)\right)\Phi(\zeta) = M^2\Phi(\zeta)\ , \tag{2}$$

where $U(\zeta)$ is the confining potential defined at equal light-front time. After identifying $\zeta$ with the co-ordinate in the fifth dimension, Eq. (2) describes the propagation of spin-$J$ string modes, in which case $U(\zeta)$ is determined by the choice for the dilaton field. We shall use the soft-wall model [10], in which

$$U(\zeta) = \kappa^4\zeta^2 + 2\kappa^2(J-1)\ . \tag{3}$$

This potential encodes the confinement dynamics of QCD and the challenge remains to derive it from first-principles QCD.

Solving Eq. (2) with this potential results in eigenvalues

$$M^2 = 4\kappa^2(n + J/2 + L/2)\ , \tag{4}$$

which reproduces the correct meson mass spectrum. In particular, it predicts a massless pion ($S = 0, n = 0, L = 0$) and $M_\rho^2 = 2\kappa^2$ for the $\rho$ meson ($S = 1, n = 0, L = 0$). The corresponding eigenfunctions are [11]

$$\Phi(\zeta) = \kappa\sqrt{2\zeta}\exp\left(-\frac{\kappa^2\zeta^2}{2}\right)\ . \tag{5}$$

It remains to specify the function $f(x)$ in Eq. (1). This can be done by comparing the expressions for the pion EM form factor obtained in the light-front formalism and in AdS space [7] and it results in

$$f(x) = \mathcal{N}\sqrt{x(1-x)}\ . \tag{6}$$

The resulting wavefunction is thus

$$\phi(x,\zeta) = \mathcal{N}\frac{\kappa}{\sqrt{\pi}}\sqrt{x(1-x)}\exp\left(-\frac{\kappa^2\zeta^2}{2}\right)\ , \tag{7}$$

where $\mathcal{N}$ is a normalisation constant. Assuming the meson is dominated by its leading $q\bar{q}$ Fock component, $\mathcal{N}$ is fixed by

$$\int \mathrm{d}^2\mathbf{b}\,\mathrm{d}x\,|\phi(x,\zeta)|^2 = \int_0^1 \frac{\mathrm{d}x}{x(1-x)} f^2(x) = 1\ . \tag{8}$$

Brodsky and de Téramond also have a prescription to account for non-zero quark masses [8]: A Fourier transform to $k$-space gives

$$\tilde{\phi}(x,k) \propto \frac{1}{\sqrt{x(1-x)}} \exp\left(-\frac{M_{q\bar{q}}^2}{2\kappa^2}\right)\ , \tag{9}$$

where the invariant mass squared of the $q\bar{q}$ pair is $M_{q\bar{q}}^2 = k^2/(x(1-x))$. For massive quarks, the invariant mass should rather be $M_{q\bar{q}}^2 = (k^2+m_f^2)(x(1-x))$. After substituting this into the wavefunction and Fourier transforming back to transverse position space, one obtains the final form of the AdS/QCD wavefunction:

$$\phi(x,\zeta) = N\frac{\kappa}{\sqrt{\pi}}\sqrt{x(1-x)}\exp\left(-\frac{\kappa^2\zeta^2}{2}\right)\exp\left(-\frac{m_f^2}{2\kappa^2 x(1-x)}\right)\ , \tag{10}$$

and $N$ is fixed by the generalization of Eq. (8):

$$\int_0^1 \frac{\mathrm{d}x}{x(1-x)} f^2(x)\exp\left(-\frac{m_f^2}{\kappa^2 x(1-x)}\right) = 1\ . \tag{11}$$

This is rather similar to the original Boosted Gaussian (BG) wavefunction discussed in [12, 13]

$$\phi^{\mathrm{BG}}(x,\zeta) \propto x(1-x)\ \exp\left(\frac{m_f^2R^2}{2}\right)\exp\left(-\frac{m_f^2R^2}{8x(1-x)}\right)\ \exp\left(-\frac{2\zeta^2}{R^2}\right)\ . \tag{12}$$

If $R^2 = 4/\kappa^2$ then the two wavefunctions differ only by a factor of $\sqrt{x(1-x)}$, which is not surprising given that in both cases confinement is modelled by a harmonic oscillator. In what follows we shall consider a parameterization that accommodates both the AdS/QCD and the BG wavefunctions:

$$\phi(x,\zeta) \propto [x(1-x)]^\beta \exp\left(-\frac{\kappa^2\zeta^2}{2}\right)\exp\left(-\frac{m_f^2}{2\kappa^2 x(1-x)}\right)\ . \tag{13}$$

## COMPARING TO DATA, QCD SUM RULES AND THE LATTICE

To compute the cross-section for $\gamma^* p \to \rho p$ we use the dipole model of high-energy scattering [14–17]. In this approach, the scattering amplitude is a convolution of the photon

and vector meson $q\bar{q}$ wavefunctions with the total cross-section to scatter a $q\bar{q}$ dipole off a proton. QED is used to determine the photon wavefunction and the dipole cross-section can be extracted from the precise data on the deep-inelastic structure function $F_2$. The details of this procedure can be found in [6, 13]. All that remains is to specify the wavefunction of the meson.

The meson's light-front wavefunctions can be written in terms of the AdS/QCD wavefunction $\phi(x,\zeta)$ [6]. For longitudinally polarized mesons:

$$\Psi^L_{h,\bar{h}}(b,x) = \frac{1}{2\sqrt{2}}\delta_{h,-\bar{h}}\left(1+\frac{m_f^2-\nabla^2}{M_\rho^2\, x(1-x)}\right)\phi_L(x,\zeta)\ , \tag{14}$$

where $\nabla^2 \equiv \frac{1}{b}\partial_b + \partial_b^2$ and $h$ ($\bar{h}$) are the helicities of the quark (anti-quark). For transversely polarized mesons:

$$\Psi^{T=\pm}_{h,\bar{h}}(b,x) = \pm[ie^{\pm i\theta}(x\delta_{h\pm,\bar{h}\mp} - (1-x)\delta_{h\mp,\bar{h}\pm})\partial_b + m_f\delta_{h\pm,\bar{h}\pm}]\frac{\phi_T(x,\zeta)}{2x(1-x)}\ , \tag{15}$$

where $be^{i\theta}$ is the complex form of the transverse separation, $\mathbf{b}$. Rather than using Eq. (11) to fix the normalization of $\phi$ we impose

$$\sum_{h,\bar{h}}\int \mathrm{d}^2\mathbf{b}\,\mathrm{d}x\,|\Psi^\lambda_{h,\bar{h}}(b,x)|^2 = 1\ , \tag{16}$$

where $\lambda = L, T$. This means we allow for a polarization dependent normalization (hence the subscripts on $\phi_{L,T}$). For longitudinal polarization, the difference between the two normalization prescriptions leads only to sub-leading differences $\sim M_\rho^2/Q^2$ or $m_f^2/M_\rho^2$ in the electroproduction scattering amplitude, where $Q^2$ is the photon virtuality. For transverse polarization, the two prescriptions lead to a slightly different normalization but this can be attributed to the ignoring of higher Fock components in the wavefunction (since all of the normalization integrals are in any case only unity up to corrections due to higher Fock components).

To compare with the HERA data we have to fix a value for the quark mass. We take $m_f = 140$ MeV, which is the value used in the fits to the deep-inelastic structure function, $F_2(x,Q^2)$ [6]. We use the CGC[0.74] dipole model [19, 20] (see [6] for details), although the predicitions do not vary much if we use other models that fit the HERA $F_2$ data [21, 22]. We also take $\kappa = M_\rho/\sqrt{2} = 0.55$ GeV, which is the AdS/QCD prediction.

Figures 1 and 2 compare the AdS/QCD predictions, shown as the solid blue curves, with the HERA data. The agreement is good and the disagreement at high $Q^2$ is not unexpected.

This is the region where perturbative evolution of the wavefunction will be relevant and the AdS/QCD wavefunction we use is clearly not able to describe that. It should be stressed that these AdS/QCD predictions are parameter-free.

We are also able to compute the electronic decay width $\Gamma_{e^+e^-}$, which is related to the decay constant via

$$f_\rho = \left(\frac{3\Gamma_{e^+e^-}M_\rho}{4\pi\alpha_{\rm em}^2}\right)^{1/2} .$$

Using

$$f_\rho = \frac{1}{2}\left(\frac{N_c}{\pi}\right)^{1/2}\int_0^1 {\rm d}x\left(1+\frac{m_f^2-\nabla^2}{M_\rho^2 x(1-x)}\right)\phi_L(x,\zeta=0)\ , \tag{17}$$

we obtain $\Gamma_{e^+e^-} = 6.66$ keV, which is to be compared with the measured value $\Gamma_{e^+e^-} = 7.04 \pm 0.06$ keV [23].

Figure 3 shows the $\chi^2$ per data point in the $(\beta,\kappa)$ parameter space (see Eq. (13)) [28]. It confirms that the AdS/QCD prediction lies impressively close to the minimum in $\chi^2$. The best fit has a $\chi^2$ per data point equal to 114/76 and is achieved with $\kappa = 0.56$ GeV and $\beta = 0.47$. Better fits to the data are possible, e.g. if one allows the parameters $\beta$ and $\kappa$ to depend on the polarization of the meson. However, given that we have not attempted to quantify the theory uncertainty we regard these as good fits. The curves resulting from the best fit are shown as the red dashed curves in Figures 1 and 2.

We have previously shown that the twist-2 Distribution Amplitude (DA) can be related to $\phi_L(x,\zeta)$ according to

$$\varphi(x,\mu) = \left(\frac{N_c}{\pi}\right)^{1/2}\frac{1}{2f_\rho}\int {\rm d}b\ \mu J_1(\mu b)\left(1+\frac{m_f^2-\nabla^2}{M_\rho^2 x(1-x)}\right)\phi_L(x,\zeta)\ . \tag{18}$$

We note that $\int {\rm d}x\ \varphi(x,\mu\to\infty) = 1$ recovers the decay constant constraint. To compare to predictions using QCD Sum Rules [24] and from the lattice [25], we can also compute the moment:

$$\int_0^1 {\rm d}x\ (2x-1)^2\varphi(x,\mu)\ . \tag{19}$$

We obtain a value of 0.228 for the AdS/QCD wavefunction, which is to be compared with the Sum Rule result of $0.24 \pm 0.02$ at $\mu = 3$ GeV [24] and the lattice result of $0.24 \pm 0.04$ at $\mu = 2$ GeV [25]. The AdS/QCD wavefunction neglects the perturbatively known evolution with the scale $\mu$ and should be viewed as a parametrization of the DA at some low scale $\mu \sim 1$ GeV. Viewed as such, the agreement is good.

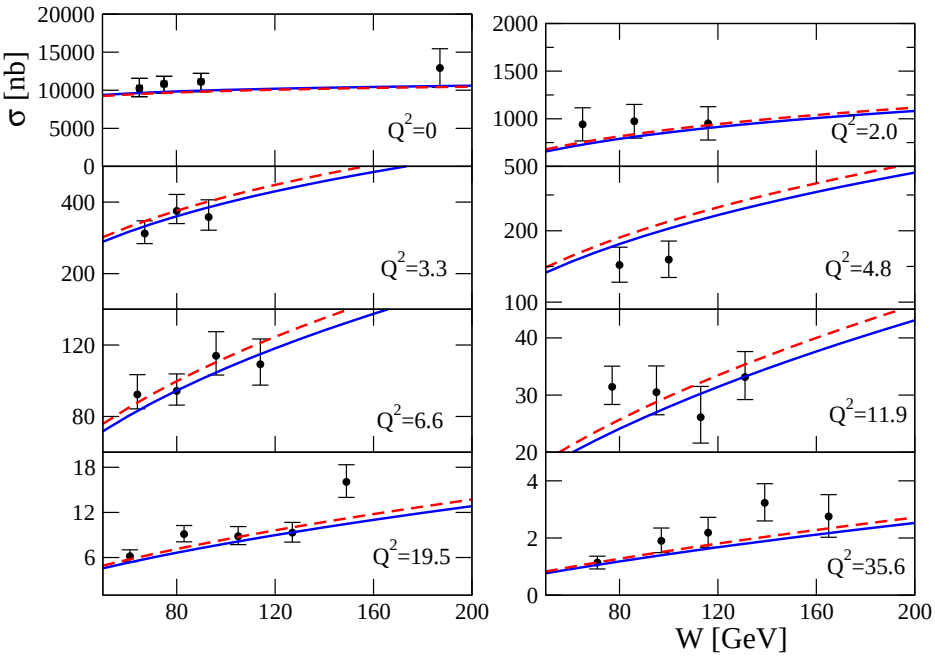


(a) H1

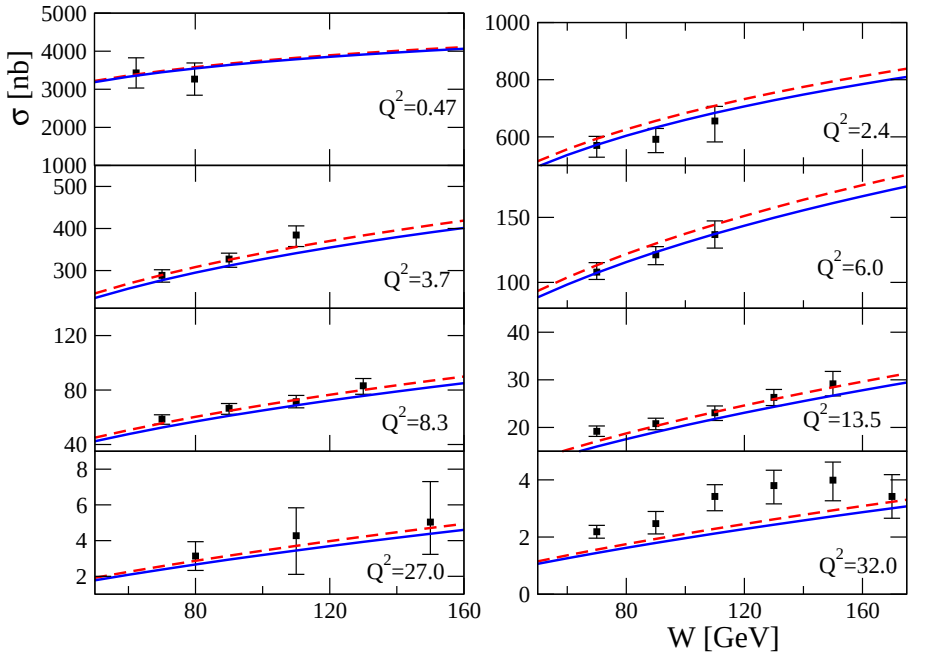


(b) ZEUS

FIG. 1: Comparison the HERA cross-section data [26, 27]. Solid blue curve is the AdS/QCD prediction and the dashed red curve is the best fit.

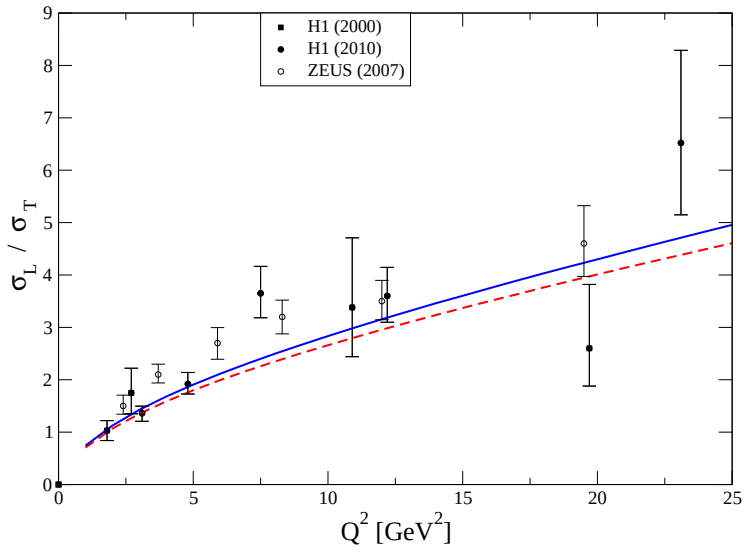


FIG. 2: Comparison to the HERA data on the longitudinal to transverse cross-section ratio [26, 27]. Solid blue curve is the AdS/QCD prediction and the dashed red curve is the best fit.

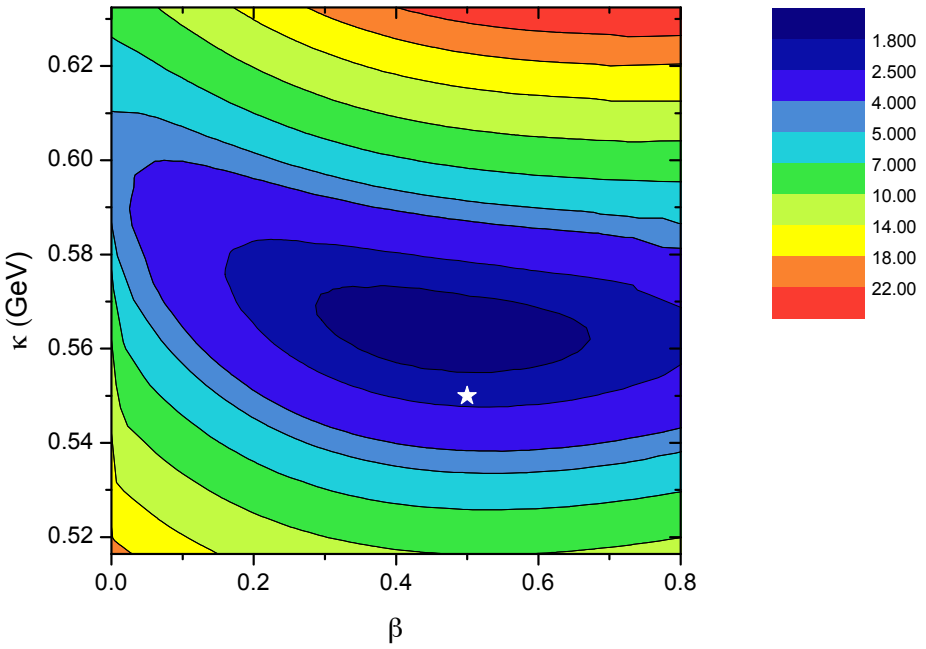


FIG. 3: The $\chi^2$ distribution in the $(\beta, \kappa)$ parameter space. The AdS/QCD prediction is the white star.

**ACKNOWLEDGEMENTS**

We thank Stan Brodsky, Mike Seymour and Guy de Téramond for their helpful comments and suggestions. The work of JRF is supported by the Lancaster-Manchester-Sheffield Consortium for Fundamental Physics under STFC grant ST/J000418/1. R.S thanks the University of Manchester and the Institute for Nuclear Theory at the University of Washington for hospitality and financial support.

* Electronic address: `jeff.forshaw@manchester.ac.uk`

† Electronic address: `ruben.sandapen@umoncton.ca`

[1] J. Erdmenger, N. Evans, I. Kirsch, and E. Threlfall, Eur.Phys.J. **A35**, 81 (2008), 0711.4467.

[2] J. Casalderrey-Solana, H. Liu, D. Mateos, K. Rajagopal, and U. A. Wiedemann (2011), 1101.0618.

[3] M. S. Costa and M. Djuric (2012), 1201.1307.

[4] G. F. de Teramond and S. J. Brodsky (2012), 1203.4025.

[5] J. R. Forshaw and R. Sandapen, JHEP **11**, 037 (2010), 1007.1990.

[6] J. R. Forshaw and R. Sandapen, JHEP **1110**, 093 (2011), 1104.4753.

[7] S. J. Brodsky and G. F. de Teramond, Phys.Rev. **D77**, 056007 (2008), 0707.3859.

[8] S. J. Brodsky and G. F. de Teramond (2008), 0802.0514.

[9] G. F. de Teramond and S. J. Brodsky, Phys.Rev.Lett. **102**, 081601 (2009), 0809.4899.

[10] A. Karch, E. Katz, D. T. Son, and M. A. Stephanov, Phys.Rev. **D74**, 015005 (2006), hep-ph/0602229.

[11] A. Vega, I. Schmidt, T. Branz, T. Gutsche, and V. E. Lyubovitskij, Phys.Rev. **D80**, 055014 (2009), 0906.1220.

[12] J. Nemchik, N. N. Nikolaev, E. Predazzi, and B. G. Zakharov, Z. Phys. **C75**, 71 (1997), hep-ph/9605231.

[13] J. R. Forshaw, R. Sandapen, and G. Shaw, Phys. Rev. **D69**, 094013 (2004), hep-ph/0312172.

[14] N. N. Nikolaev and B. G. Zakharov, Z. Phys. **C49**, 607 (1991).

[15] N. N. Nikolaev and B. G. Zakharov, Z. Phys. **C53**, 331 (1992).

[16] A. H. Mueller, Nucl. Phys. **B415**, 373 (1994).

[17] A. H. Mueller and B. Patel, Nucl. Phys. **B425**, 471 (1994), hep-ph/9403256.

[18] J. R. Forshaw and R. Sandapen (2010), 1012.4956.

[19] G. Soyez, Phys. Lett. **B655**, 32 (2007), 0705.3672.

[20] G. Watt and H. Kowalski, Phys. Rev. **D78**, 014016 (2008), 0712.2670.

[21] J. R. Forshaw and G. Shaw, JHEP **12**, 052 (2004), hep-ph/0411337.

[22] H. Kowalski, L. Motyka, and G. Watt, Phys. Rev. **D74**, 074016 (2006), hep-ph/0606272.

[23] Particle Data Group, J. Phys. **G37**, 075021 (2010).

[24] P. Ball, V. M. Braun, and A. Lenz, JHEP **08**, 090 (2007), 0707.1201.

[25] P. A. Boyle et al. (RBC), PoS **LATTICE2008**, 165 (2008), 0810.1669.

[26] S. Chekanov et al. (ZEUS), PMC Phys. **A1**, 6 (2007), 0708.1478.

[27] The H1 Collaboration, JHEP **05**, 032 (2010), 0910.5831.

[28] We include the electroproduction data and also the decay constant $f_\rho$ in the fit.